The behavior of hydrogen on Nb, and possibly several other transition metals, can be qualitatively understood with use of the simple thermodynamic model which was recently solved to explain hydrogen uptake by Nb.[8] In this model the surface and bulk concentrations of hydrogen are in equilibrium, with the relative concentrations depending on temperature and the difference between the heat of solution and the heat of desorption. When the difference is small the hydrogen moves more readily into the bulk and the surface must be cooled to "freeze in" the surface coverage. For Nb at room temperature the hydrogen is in the near-surface region but has some equilibrium distribution trailing into the bulk. In this picture, the meaning of "surface region" is crucial since Ti and Pd are stated to have two-dimensional adlayers of hydrogen[2,6] while the results presented here show this not to be the case for Nb at room temperature. It is apparent that the model in Ref. 8 should be modified to include a "near-surface" distribution, and that the studies presented here suggest a means of further understanding the interaction of hydrogen with transition-metal surfaces.

[1]T. E. Felter, R. A. Barker, and P. J. Estrup, Phys. Rev. Lett. 38, 1138 (1977); M. K. Debe and D. A. King, J. Phys. C 10, L303 (1977).

[2]S. G. Louie, Phys. Rev. Lett. 42, 476 (1979).

[3]P. J. Feibelman and D. R. Hamann, Phys. Rev. B 21, 1385 (1980); P. J. Feibelman, D. R. Hamann, and F. J. Himpsel, Phys. Rev. B 22, 1734 (1980).

[4]S.-L. Weng and M. El-Batanouny, Phys. Rev. Lett. 44, 612, 903(E) (1980), and references therein.

[5]J. E. Demuth, Surf. Sci. 65, 369 (1977).

[6]E. W. Plummer, unpublished.

[7]R. J. Smith, Phys. Rev. B 21, 3131 (1980).

[8]M. A. Pick, J. W. Davenport, M. Strongin, and G. J. Dienes, Phys. Rev. Lett. 43, 286 (1979).

[9]R. J. Smith, G. P. Williams, J. Colbert, M. Sagurton, and G. J. Lapeyre, Phys. Rev. B 22, 1584 (1980).

[10]Since no comprehensive data were found for Nb, I used the results for hot electrons in Cu from J. A. Knapp, F. J. Himpsel, and D. E. Eastman, Phys. Rev. B 19, 4952 (1978).

Saturation of the Image Potential Observed in Low-Energy Electron Reflection at Cu(001) Surface

R. E. Dietz, E. G. McRae, and R. L. Campbell

Bell Laboratories, Murray Hill, New Jersey 07974

High-resolution low-energy electron-diffraction measurements of the (00) beam from Cu(001) are reported. Fine structure near the (11) beam threshold is explained by an interference between the directly reflected wave and a wave internally reflected at the surface potential barrier. With use of this interpretation, the observed lineshapes have been fitted by adjusting two parameters describing the shape of the potential. It is concluded that the long-range potential saturates to a value about one-half the crystal inner potential.

PACS numbers: 73.20.Cw

The shape of the potential acting on electrons near a metal surface is a fundamental question that has long attracted theoretical interest.[1-3] At large distances z from the surface, the potential $U(z)$ has the "image" form $-1/4(z - z_0)$ (Hartree atomic units), where z_0 denotes the image-potential origin. For decreasing distances in the near region $z \approx z_0$ the potential is progressively weaker than the image potential and eventually approaches the inner potential of the metal. The saturation of the image potential has been described theoretically for certain hypothetical cases, (e.g., stationary electrons) but no calculations for realistic models nor experiments bearing on this top-

ic have been reported. In this paper we show that the saturation of the image potential can be observed in high-resolution low-energy electron-diffraction (LEED) experiments. The specific result is that for 10-eV electrons travelling almost parallel to the Cu(001) surface, the lateral potential in the near region $z \approx z_0$ is nearly linear and extrapolates at the surface to a value about one-half that of the inner potential. The larger implication is that experiments of this type promise a check of theory for models of the interaction of electrons with metal surfaces.

Our approach centers on the Rydberg-like LEED intensity fine structure that is observed in narrow energy ranges just below the thresholds of diffracted beams. Jenning and co-workers[4,5] and others[6] have shown that this fine structure might be interpreted to verify the image form of the potential in the far region $z \gg z_0$ and to determine the image-potential origin z_0. The present program consists of measurements with sufficiently high resolution and analysis with sufficient precision to trace the shape of the potential into the near region where the image potential saturates.

The physical mechanism underlying our analysis has been described as part of a general theory of LEED.[7,8] A simplified form of it is shown schematically in Fig. 1. Figure 1 refers specifically to the (00) beam in the vicinity of the threshold for the gth diffracted beam. The essential element of the mechanism is "indirect" reflection involving a "preemergent" beam—i.e., a beam whose surface normal momentum is slightly less than required for grazing emergence. The indirect processes consist of (1) diffraction into the pre-emergent beam traveling almost parallel to the surface, (2) multiple scattering of the pre-emergent beam between the substrate and surface potential barrier, and (3) diffraction from the preemergent to an outgoing propagating beam. By summing the geometric series in the reflection amplitudes at the right of Fig. 1, we get an expression for the total reflection amplitude T_{00}:

$$T_{00} = T_{00}{}^o \left[1 + \frac{R S_{gg}}{1 - T_{gg}{}^o S_{gg}} \right].$$ (1)

The second term in the brackets is the ratio of the indirect amplitude contribution to the "direct" contribution $T_{00}{}^o$ that is due to single reflection at the substrate. Symbols S_{gg} and $T_{gg}{}^o$ denote amplitude coefficients of specular reflection of the preemergent beam at the surface potential barrier and substrate, respectively, while $R = T_{0g}{}^o T_{g0}{}^o / T_{00}{}^o$ denotes the product of diffraction amplitudes
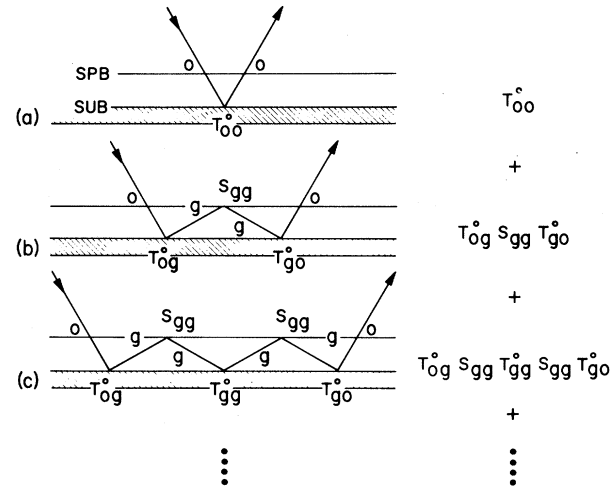

FIG. 1. Physical mechanism of threshold structure in LEED (schematic). The figure refers to the (00) beam in the vicinity of the threshold for the gth diffracted beam. In each panel the horizontal lines represent the surface potential barrier and substrate, respectively. Panel (a) represents direct reflection and the other panels represent indirect reflection processes. Arrows marked 0 indicate the incident and specularly reflected beams. Arrows marked g indicate preemergent beams. The expressions at the right are contributions to the amplitude T_{00} from the corresponding reflection processes. Amplitude coefficients of transmission and reflection of the 0th beam at the surface potential barrier are taken in a simplifying assumption to be 1 and 0, respectively. Summation over these amplitude contributions gives Eq. (1) in the text.

into and out of the preemergent beam, divided by the direct reflection amplitude.

The existence of sequences of LEED peaks near beam thresholds derives essentially from variation of the phase $\arg S_{gg}$ of the surface potential barrier reflection amplitude S_{gg} in Eq. (1). Approaching the threshold, the phase varies increasingly rapidly as a function of electron energy E and reduced parallel momentum $\vec{k}_{\parallel}$. This rapid phase variation arises from the long-range character of the potential. It is quite sensitive to the shape of the surface barrier. Therefore, the barrier shape can be determined by trial fits to observed LEED line shapes with use of intensities $|T_{00}|^2$ as given by Eq. (1) with phases calculated for assumed barrier shapes.

Measurements of the elastic specularly reflected current of electrons from Cu(001) were carried out using a low-energy scattering spectrometer equipped with a 127° cylindrical-sector electrostatic monochromator and analyzer. Meas-

urements of the specularly scattered beam current were made for polar angles $25° \le \theta \le 85°$, along both (11) and (10) azimuths. The energy and angular widths of the incident beam were less than 20 meV and $0.5°$, respectively. A typical spectrum (points) is shown in Fig. 2. Small ambient magnetic and electrostatic fields tended to deflect the beam across the entrance aperature of the analyzer as E was scanned over intervals > 1 eV. This caused an apparent energy dependence of the sensitivity of the measurement. To compensate in part for the resulting distortion of the line shape we have separately normalized the data above and below 12 eV.

In applications of Eq. (1) to LEED results for Cu(001) surface such as those of Fig. 2, we have consistently found that the best fits to the data are obtained with $T_{gg}{}^0$ equal to zero. This means that the resonance effect deriving from the variation of the denominator $1 - T_{gg}{}^0 S_{gg}$ in Eq. (1) is quite unimportant in the present instance. Aside from putting $T_{gg}{}^0 = 0$, we also find from fitting Eq. (1) that R is independent of $(E, \vec{k}_{\parallel})$ over the range of the experiment. The surface barrier potential
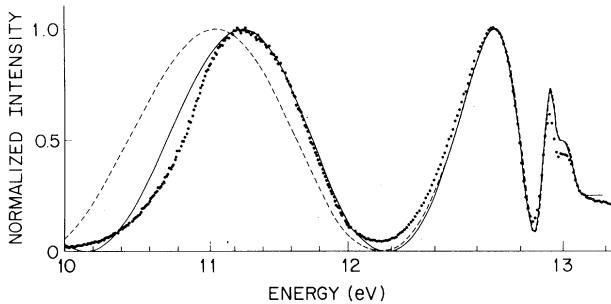
is assumed one dimensional, so that $\arg S_{gg}$ depends on $\epsilon = E - E_\infty(\vec{k}_{\parallel})$, where E_∞ is the threshold energy, rather than on E and $\vec{k}_{\parallel}$ independently. We assume that $|S_{gg}|$ has a constant value for $\epsilon < 0$ and is zero for $\epsilon > 0$.

The form of potential $U(z)$ adopted to fit the data is linear for $z \approx z_0$ and joins smoothly to the image form for larger z. Its intercept $U(0)$ is in general different from the inner potential $-U_0$ (see Fig. 3, inset). The potential is characterized by the two parameters $U(0)$ and z_0. The vertical drop of the potential to $-U_0$ at $z = 0$ is an obviously unrealistic property of the assumed potential that does not, however, have any important bearing on the present results. It does not contribute to the calculated value of $\arg S_{gg}$. Corrections allowing the potential to drop smoothly to $-U_0$ may be important for calculating intensities far from threshold, but we find that in fitting with both linear and quadratic terms the linear term is dominant for the energy range shown in Fig. 2. The origin $z = 0$ is defined as the plane on which

FIG. 2. Specularly reflected current from Cu(001) surface, plotted as a function of incident energy: (11) azimuth, polar angle $\theta = 61.7°$. Points: experimental data normalized as described in the text. Note the change of scale at 12.0 eV. Lines: calculations by Eq. (1) (text) with use of the straight-line continuation to the image potential with $z_0 = 3.8$ a.u., $U(0) = -7$ eV, $\arg R = 1.38\pi$ (full line) and $z_0 = 3.0$ a.u., $U(0) = -7$ eV, $\arg R = 1.65\pi$ (broken line). In both cases $|RS| = 1.0$ and $|T_{gg}{}^0| = 0$. The fitting proceeded by choosing $|RS|$ so as to give the correct peak to background intensity ratio. Then for a given choice of z_0, $\arg R$ was adjusted to bring a calculated peak into agreement with the experimental one at 12.7 eV. Then $U(0)$ was adjusted to fit the position of the lowest-energy peak. The validity of the model potential is confirmed by the agreement of the resulting shapes. The expected Rydberg series near threshold is broadened into an error function by convoluting with a Gaussian of 0.050 eV width, which reflects the experimental spread in both energy and momentum.
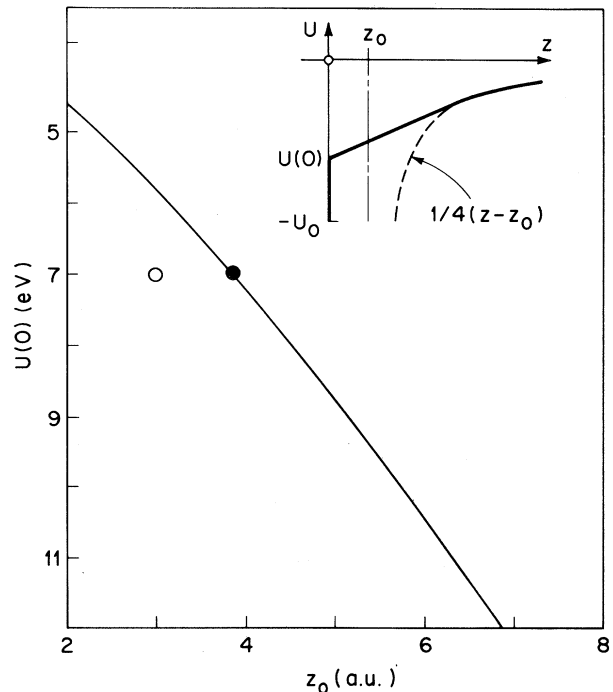

FIG. 3. The range of values of the surface-barrier shape parameters z_0 and $U(0)$ that give a good fit to the data of Fig. 2 (line) and the values used in calculating the curves shown in Fig. 2 (circles). The solid and open circles refer, respectively, to the full and broken curves in Fig. 2. The inset shows the assumed form of potential (full line) and the image potential (broken line).

$d(\arg R)/dE = 0$. In two-beam diffraction theory for a range of $(E, \vec{k}_{\parallel})$ outside any band gap, this plane is the same as the positive–charge-density boundary in the jellium model.[9] The energy independence of $\arg R$ is confirmed by experiment as discussed below.

We have also tried a potential introduced in this context by Jennings.[4,5] This potential is essentially an image potential which is truncated to a flat potential at $U = -U_0$. In using this form for the potential barrier, we have not been able to compute reflectivity spectra in agreement with our experimental data.

In all cases $\arg S_{gg}$ was calculated by numerical integration of the Schrödinger equation for the potential $U(z)$ followed by matching of the solution at $z = 0$ to the superposition of plane waves $e^{i\kappa z} + S_{gg}e^{-i\kappa z}$, where $\kappa \equiv \{2[\epsilon - U(0)]\}^{1/2}$.

Figure 2 shows reflectivity curves calculated for two slightly different potentials of the type shown in Fig. 3, inset. The values of the potential parameters $U(0)$ and z_0 used in calculating the full and broken curves in Fig. 2 are indicated in Fig. 3 by the solid and open circles, respectively.

The full curve in Fig. 2 represents very nearly the best fit to experiment that can be obtained with the present model. An equally good fit is obtained for all $[U(0), z_0]$ values on the line in Fig. 3. This "best-fit" line thus summarizes all potentials (Fig. 3, inset) that reproduce the experimental line shape.

The sensitivity of the line shape to departures from the "best-fit" line (Fig. 3) is indicated by the difference between the full and broken curves in Fig. 2. For energies close to the threshold, the line shape is insensitive to changes of $U(0)$ or z_0. This insensitivity is due in part to our procedure of adjusting $\arg R$ to keep one of the peak positions constant. But the absence of any residual dependence on $U(0)$ or z_0 and the extremely good fit to experiment indicate that for energies close to threshold the line shape depends primarily on the potential at large distances where the image form [Eq. (1)] applies. The opposite situation applies for energies near the lowest-energy peak and relatively far from threshold. As illustrated in Fig. 2, the line shape near the lowest-energy peak depends sensitively on variations of $U(0)$ or z_0 which in our model describe the shape of the potential close to the surface.

We have verified that the results summarized by the "best-fit" line in Fig. 3 are a property of the potential only and do not derive from any sys-

tematic variation of R with electron energy. This result was obtained by examining data similar to that of Fig. 2 taken over the entire angle range of observation. The corresponding range of threshold energies is 12–20 eV. In all of these data, the line shape up to the second resolved peak from threshold was independent of the threshold energy. This is possible in our description only if R and also z_0 are independent of energy.

Our conclusion (Fig. 3) is that the potential lies between the following limits: (a) $|U(0)|$ is much smaller than the inner potential (about 12 eV for Cu; (b) z_0 is much larger than theoretical estimates of the distance of the average-potential origin from the jellium boundary for static models of simple metals (1–2 a.u. for Al).[2] A separate theoretical calculation of $\arg R$, such as has been carried out by Jennings and co-workers,[4,5] would be needed to locate the potential between these limits. However, considerations of the dependence of the potential on the electron velocity favor a description close to limit (a). In the present experiments the surface-barrier potential is sensed by an electron traveling almost parallel to the surface with kinetic energy several times the plasma energy of Cu. Thus the long-range part of the potential ought to saturate to a value much smaller than the inner potential. On the other hand the value of z_0 is independent of electron velocity and should not be grossly different from theoretical estimates for static models.

Our observation of the saturation of the image potential calls for an extension of existing theory to describe the potential acting on electrons traveling almost parallel to metal surfaces as in pre-emergent LEED beams. We anticipate that such theory will describe not only the z dependence of the potential but also its dependence on the electron energy and surface-parallel momentum. Experiments are in progress to follow the energy and momentum dependence of the potential for both Al and Cu surfaces, and to extend the measurements farther from the threshold so as to probe the shape of the potential closer to the surface.

---

[1]D. M. Newns, J. Chem. Phys. 50, 4572 (1969), and Phys. Rev. B 1, 3304 (1970).

[2]J. A. Appelbaum and D. R. Hamann, Phys. Rev. B 6,

1122 (1972); N. D. Lang and W. Kohn, Phys. Rev. B 7, 3541 (1973); A. G. Eguiluz, Solid State Commun. 33, 21 (1980).

[3]J. Heinrichs, Phys. Rev. B 8, 1346 (1973); G. D. Mahan, in *Proceedings of the Twenty-Fourth Nobel Symposium on Collective Properties of Physical Systems, Aspenaasgarden, Sweden, 1973*, edited by B. Lundqvist and S. Lundqvist (Academic, New York, 1974), p. 164; J. Harris and R. O. Jones, J. Phys. C 6, 3585 (1973); J. Harris and R. O. Jones, J. Phys. C 7, 3751 (1974); C. H. Hodges, J. Phys. C 8, 1849 (1975); M. Jonson, Solid State Commun. 33, 743 (1980).

[4]M. N. Read and P. J. Jennings, Surf. Sci. 74, 54

(1978); P. J. Jennings, Surf. Sci. 75, L773 (1978); P. J. Jennings and G. L. Price, Surf. Sci. 93, L124 (1980).

[5]G. L. Price, P. J. Jennings, P. E. Best, and J. C. L. Cornish, Surf. Sci. 89, 151 (1979).

[6]A. Adnot and J. D. Carette, Phys. Rev. Lett. 38, 1084 (1977); A. Adnot and J. D. Carette, Phys. Rev. B 16, 4703 (1977); J. Rundgren and G. Malmström, Phys. Rev. Lett. 38, 836 (1977); J. Rundgren and G. Malmström, J. Phys. C 10, 4671 (1977); J. B. Pendry and P. M. Echenique, J. Phys. C 11, 2065 (1978).

[7]E. G. McRae, Surf. Sci. 25, 491 (1971).

[8]E. G. McRae, Rev. Mod. Phys. 51, 541 (1979).

[9]E. G. McRae, Surf. Sci. 47, 167 (1975).

Enormous Yield of Photoelectrons from Small Particles

A. Schmidt-Ott

Laboratory for Atmospheric Physics[a] and Laboratory for Solid State Physics, Eidgenössische Technische Hochschule, CH-8093 Zürich, Switzerland

and

P. Schurtenberger and H. C. Siegmann

Laboratory for Solid State Physics, Eidgenössische Technische Hochschule, CH-8093 Zürich, Switzerland

(Received 7 July 1980)

A new ac bridge technique allows detailed photoelectric studies on very small particles suspended in gases. The photoelectric yield Y near threshold Φ still follows the Fowler-Nordheim law $Y = c(h\nu - \Phi)^2$; yet c is generally much larger compared to surfaces of extended solids. For Ag particles of radius 20 Å in an airlike mixture of N_2 and O_2, $c \simeq 100 c_0$, where c_0 applies to a macroscopic Ag surface in the same environment.

The purpose of this Letter is to report on a large enhancement of the yield Y of photoelectrons per incident photon if ultrafine particles with radii $R \lesssim 50$ Å are chosen as photoemitters. The results were obtained with Ag and WO_3 by use of a novel technique in which the density Z of the particles does not have to be known.

The particles are suspended in an N_2-O_2 mixture similar to air. The photoelectric size effect to be reported here has wide implications including photoemission from interstellar dust grains by starlight,[1] atmospheric electricity,[2] nucleation,[3] and smog photochemistry,[3,4] simply because photoemission from small particles has been underestimated so far. It also may become the physical basis for characterizing and measuring very small particles suspended in gases.

For the determination of Y and the particle radius R, the aerosol is illuminated with monochromatic light from a Xe high-pressure arc and the conductivity arising from photoelectron emission by the particles is measured. For this photo-conductivity measurement an alternating electric field (amplitude, 30 V/cm; frequency, 90 s^{-1}) is applied to the aerosol in two cylindrical condensers, one of which is exposed to uv light. Here, an in-phase current component is caused by the oscillatory motions of the charge carriers produced by photoemission.[5] The differential conductivity in the two condensers is measured in an ac bridge circuit by means of a phase-sensitive amplifier.[5] In this way, the capacitive component, typically 10^6 times higher than the photoconductivity, can be suppressed and the aerosol conductivity arising from ionization by cosmic rays and natural radioactivity is eliminated.

Aerosol photoconductivity Σ arises from the negative small ions formed by the photoelectrons[6] and the particles left behind with a positive charge. With ultrafine particles ($R \lesssim 30$ Å), small ion reattachment is negligible.[7] Multiple photoelectric particle charging can also be neglected with the low photon energies applied here, because of the strong Coulomb attraction between a doubly